Biomedical Signal Processing and Control 81 (2023) 104438

Contents lists available at ScienceDirect

Biomedical Signal Processing and Control

journal homepage: www.elsevier.com/locate/bspc

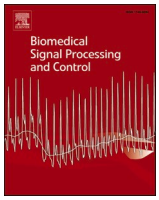

Filtering strategies of electrocardiographic imaging signals for stratification of atrial fibrillation patients

Rubén Molero *, Ismael Hernández-Romero, Andreu M. Climent, María S. Guillem

COR Group - ITACA Institute, Universitat Politècnica de València, Valencia, Spain

ARTICLE INFO

Keywords:
Atrial fibrillation
Electrocardiographic imaging
Inverse problem
Rotors
Signal processing

ABSTRACT

Background and objective: Electrocardiographic imaging (ECGI) has been used for guiding atrial fibrillation (AF) ablation, identifying reentrant activity by phase analysis with promising results. The objective of this study is to identify the best post-processing configuration for reentrant activity detection that better differentiates AF patients with different prognoses after catheter ablation.

Methods: ECGI signals of 24 AF patients before pulmonary vein isolation (PVI) were recorded. Patients were classified based on recurrence 6 months after PVI. Reentrant metrics were compared using 3 types of post-processing: none, sinusoidal recomposition (SRC), and narrow band-pass filtering centered at the highest dominant frequency (NB HDF). Different thresholds for rotor duration were also compared (0.5, 1, and 1.5 turns).

Results: The use of raw ECGI signals with a threshold of 1 turn presented the optimal processing to identify PVI-positive responders ($p < 0.05$). NB HDF showed a better ability to find statistical differences between patients than SRC.

Conclusion: Aggressive filtering of AF ECGI signals does not improve rotor identification to predict PVI outcome. Restrictive rotor duration thresholds diminish patient stratification. This definition of a post-processing strategy that allows patient stratification can be used for the improvement of the standard of care for finding the best candidates for PVI.

1. Introduction

Atrial fibrillation (AF) is the most common cardiac arrhythmia, and maintenance can be partially attributed to drivers that cause reentrant electrical activity on the surface of the atria [1]. This arrhythmia can be terminated by invasive procedures like pulmonary vein isolation (PVI), an ablation procedure that has been shown to be effective for restoring sinus rhythm. Prior studies have shown that ablation of reentrant drivers and/or focal sites improves the results of the ablation procedures as compared to PVI only [2,3]. Identifying these reentrant patterns with current invasive mapping technologies is challenging, and for this reason, noninvasive alternatives that offer a panoramic view of both atria, i.e., electrocardiographic imaging (ECGI), can be useful for the identification of AF drivers. ECGI allows estimating the epicardial electrical activity by using body surface electrocardiograms and the information of the anatomy of the patient. Several studies have made use of ECGI to guide ablation procedures in patients with AF [3,4] with promising results.

With the objective of validating ECGI signals during AF, we have shown that complexity metrics of propagation patterns of intracardiac and ECGI mapping in AF patients are correlated [5]. However, it is still unknown the relevance of either a lack of accuracy of ECGI, poor accuracy of the intracardiac mapping technology with a limited spatial resolution and areas that cannot be mapped by basket catheters, or a poor post-processing strategy for rotor identification on the discrepancies observed between ECGI and electrogram mapping metrics during AF. Likewise, an agreed strategy of how to post-process ECGI signals is not defined to evaluate the reentrant activity of AF; thus, in this article,

Abbreviations: AF, Atrial Fibrillation; AUC, Area Under the Curve; BSPM, Body Surface Potential Mapping; ECGI, Electrocardiographic Imaging; NB HDF, Narrow Band filter at Highest Dominant Frequency; PVI, Pulmonary Vein Isolation; ROC, Receiver Operating Characteristic Curve; SP, Singularity Point; SRC, Sinusoidal Recomposition.

* Corresponding author.
E-mail addresses: rumoal1@itaca.upv.es (R. Molero), isherro@itaca.upv.es (I. Hernández-Romero), acliment@itaca.upv.es (A.M. Climent), mguisan@itaca.upv.es (M.S. Guillem).

https://doi.org/10.1016/j.bspc.2022.104438
Received 13 June 2022; Received in revised form 28 October 2022; Accepted 20 November 2022
Available online 2 December 2022

we compare different strategies to evaluate rotor identification.

Rotors are typically identified by phase mapping after computing the Hilbert transform of ECGI signals [6–8]. Hilbert transform allows finding an instantaneous correspondence between the time series of an ECGI signal into phases of the activation sequence. Singularity Points (SP) are sites where a propagation pattern pivots around and are found as sites where all phases converge. In previous studies using physiological computer models of AF, we have shown that connected SPs should be required to complete at least one turn to be considered as rotors in order to achieve enough specificity [9]. However, this threshold has not been validated with human data, in which far field contributions still present after solving the inverse problem do result in tracking discontinuities in rotor detection. Under these uncertainties that occur in real patient data, real rotors lasting for several turns can be incorrectly detected as multiple rotors lasting less than one turn and, therefore, a too restrictive threshold may result in a lack of sensitivity.

In order to improve potential limitations of sensitivity in the detection of rotors, several post-processing filtering approaches have been proposed: none, sinusoidal recomposition filtering [10], and filtering the signals with a narrow band-pass filter centered at the highest dominant frequency [9]. The objective of the present study is to identify which are the best post-processing techniques to identify atrial rotors, including both the filtering strategy employed for conditioning the ECGI signals and the number of turns required for SPs to be considered as rotors. We will base our selection criteria on maximizing the differences in the variability of rotor metrics of patients with a favorable and unfavorable outcome after pulmonary vein isolation (PVI), under the assumption that the underlying electrical characteristics of these two groups of patients should be different and identifiable by ECGI. Furthermore, we hypothesized that the variability of reentrant metrics should be lower in patients with good PVI outcome. A preliminary version of this work has been reported [11].

2. Methods

2.1. Patient signal and geometry acquisition

Signals from 24 AF patients (18 females and 6 males; 61.8 ± 14.3 years old) were obtained by Body Surface Potential Mapping (BSPM) with 57 electrodes placed on the torso surface prior to a wide circumferential PVI procedure [12]. Patients gave informed consent, and the protocol was approved by the Ethics Committee of Hospital Gregorio Marañón, Madrid, Spain (reference 475/14). Two groups of patients were defined according to the success of PVI 6 months after the intervention: patients with sinus rhythm after 6 months (N = 13), and patients with atrial arrhythmia after 6 months (recurrence of AF, atrial tachycardia, or atrial flutter, N = 11).

The torso geometry of the patients and the electrode location were obtained using video recording and reconstructed by photogrammetry techniques [13]. MRI/CT scan images were also obtained, and both the atria and the torso were segmented using ITK-SNAP software [14]. Torso and atrial geometries were co-registered using the torso reference from MRI/CT images.

BSPM signals were recorded at 57 locations on the torso with 0.05 to 500 Hz filtering and a sampling frequency of 1 kHz [5]. Two signals per patient were segmented (4 ± 0.31 s) and then band-pass filtered between 2 and 45 Hz to eliminate noise, and ventricular activity (QRST segment) was canceled lead by lead by Principal Component Analysis (PCA) approach [15]. Inverse computed electrograms (ECGI) of each BSPM signal were calculated by using zero-order Tikhonov regularization and L-curve optimization [16].

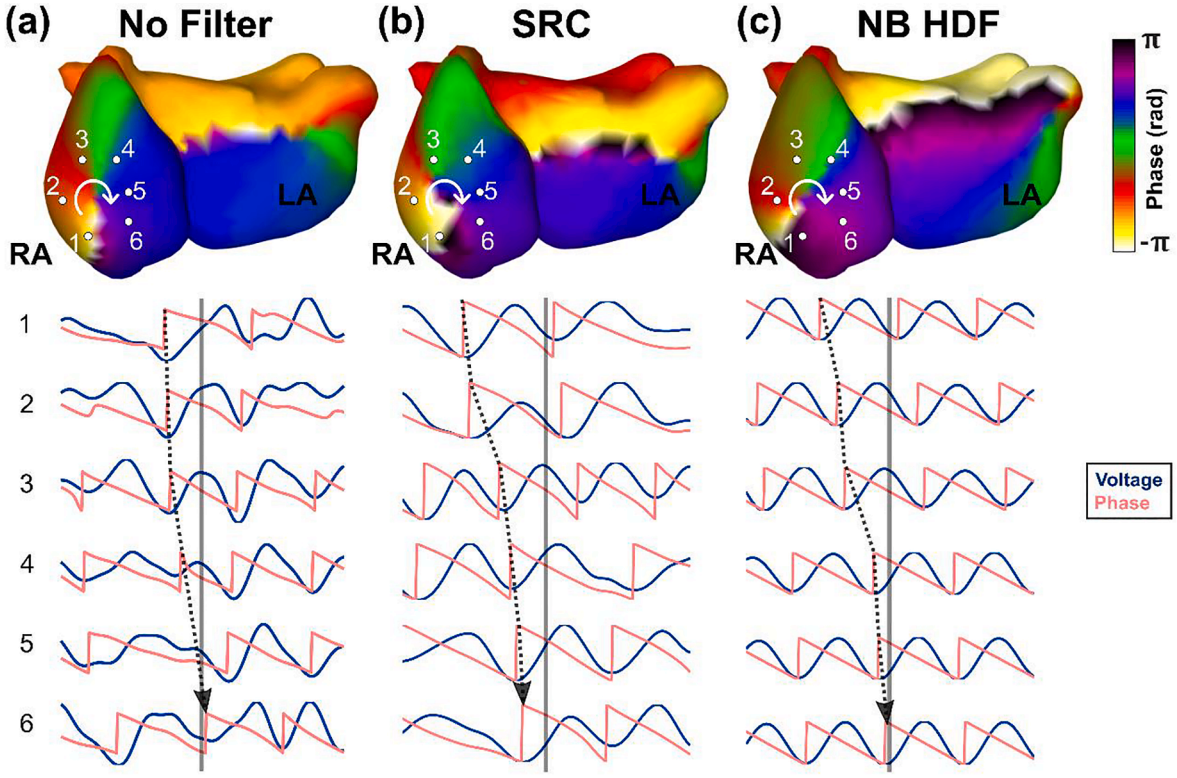

Fig. 1. Example of consecutive ECGI signals around a phase singularity for each type of processing (no filter, sinusoidal Recomposition (SRC), and narrow band-pass filter at the highest dominant frequency (NB HDF). Blue signals represent the voltage value, and pink signals the phase obtained with Hilbert's transform. Solid line on top of the electrograms represents the time instant chosen for representation in the phase maps depicted and dotted line represents the course of the reentry, most evident in the transition of phases between -π and π. (For interpretation of the references to color in this figure legend, the reader is referred to the web version of this article.)

2.2. ECGI post-processing

With the objective of adequately identifying AF drivers, 3 ECGI signal processing alternatives, Fig. 1, were applied before phase calculations were computed. Metrics based on raw ECGI signals (no further filtering or other post-processing) were compared with the same signal with two different filters, namely sinusoidal recomposition (SRC) and narrow band-pass filtering (NB HDF).

- Sinusoidal Recomposition (SRC) [10] consists of decomposing each signal into a set of sinusoidal wavelets with an amplitude proportional to the slope of the signal at a given time instant, Fig. 1(b). The period of the wavelet is computed as the mean cycle length of each ECGI signal derived from the dominant frequency of the electrogram. Welch's periodogram was calculated to obtain the power spectral density of electrograms using a 2000 ms window.

- Narrow band-pass filtering centered at the Highest Dominant Frequency (NB HDF) was applied to ECGI signals with a bandwidth of 1 Hz (HDF $\pm$ 0.5 Hz), Fig. 1(c). HDF was calculated as the 95 percentile of the dominant frequency of all ECGI signals together. To obtain dominant frequencies, the power spectral density was computed by Welch's periodogram as in previous works [9,17].

2.3. Reentrant activity detection

The instantaneous phase of ECGI signals was computed using Hilbert's transform [7]. This transform allows assigning a value between -π and + π to each sample of the signal. The reentrant atrial activity was defined as a phase progression from -π to + π monotonically increasing or decreasing around a single point in the epicardium. Singularity points (SP) were required to be identified in at least two of three concentric rings [9]. To consider a SP as a rotor, three different temporal thresholds were compared: 0.5, 1, and 1.5 turns. As a result of this thresholding criteria, nine alternatives: 3 filtering strategies and 3 different rotor duration thresholds, were evaluated. Furthermore, for each alternative SPs histograms were calculated to represent the cumulative SPs in each node of the atria surface.

2.4. Reentrant activity evaluation and statistical analysis

To evaluate each rotor detection alternative, different metrics were calculated. First, in order to make our SP detection independent of the sampling frequency, we quantified the amount of singularity points per time unit (SP/ms). The mean duration of rotors was also computed as the mean duration of detected rotors. Finally, the Shannon entropy of the SP histogram was calculated. The maximum displacement of each rotor was also calculated as the maximum distance between two phase singularities of the same rotor.

The mean value of metrics extracted from two segments of signals from the same patient was calculated for each post-processing alternative. To study the variability in time of the metrics, the absolute difference between metrics extracted from both signal segments was computed and calculated for the totality of the patients for each post-processing case: ΔSP/ms, ΔRduration and ΔEntropy.

To detect if there are significant differences in the variability of metrics extracted from two ECGI signals and between the two groups of patients (PVI responders or nonresponders with bad outcome), the normality of the values was studied using the Kolmogorov-Smirnov test followed by Student's *t*-test with normal samples and Wilcoxon rank-sum test to non-normal samples for each post-processing alternative.

For a more comprehensive evaluation of the ability to identify each patient group, a metric derived from the three presented metrics was computed, normalizing each of the metrics based on their minimum and maximum value and averaging them. Univariate logistic regression of this overall ratio was calculated for each of the post-processing techniques to quantify the ability to discriminate between patient groups. Receiver operating characteristic curves (ROC) of each case was computed as well as the resultant area under the curve (AUC). Furthermore, confusion matrices of each logistic regression were obtained using the optimal operating point of the ROC curve as a threshold.

3. Results

3.1. Reentrant activity analysis

In Fig. 2, an example of the effect of the different rotor detection alternatives is presented. Phase maps of the same patient at the same time instant for the 9 studied alternatives are shown. As it can be observed, the different filtering strategies do impact the phase distribution, and, therefore, rotors are identified at different locations even for the same time instant. With the less restrictive rotor duration threshold, we can observe differences between the different filtering strategies. Using raw signals, the number of short-lasting detected rotors is large because either they represent short changes in the direction of the phase that show an altered substrate or the tracking may be lost at several time frames. SRC resulted in fewer detected rotors mostly at the same locations as those detected with the raw signals, but also short-lasting. NB HDF filtering shows longer-lasting rotors and at similar locations than for the raw signals.

Restrictions on rotor duration do have an impact on the location of the detected rotors since short-living rotors or rotors that disappear transiently are not considered, which is more evident for a 1.5 turns threshold: both raw and SRC do not present rotors meeting this temporal restriction.

In Fig. 3, a summary of SP identification over a segment for the same patient depicted in Fig. 2 is illustrated. All the maps clearly show the presence of reentrant activity in the pulmonary veins and the lower part of the right atrium. Rotor histograms obtained after SRC and raw signals are very similar to each other for any rotor duration threshold. NB HDF maps show a larger amount of SPs detected compared with the other two types of processing techniques. It can be observed a decreased rotor detection when the rotor duration threshold is more restrictive (higher number of turns) for no filtered and SRC histogram maps. Despite the detection of fewer amount of rotors with a higher turn threshold, the area where the rotors anchor was preserved. On the contrary, maps with 0.5 turns as the threshold showed an increased reentrant activity that may be caused by the consideration of areas of lower changes in phase as SPs.

Temporal evolution of rotor detection with the different strategies presented is depicted in Fig. 4, where each row in each panel represents a rotor, and the vertical axis represents time. The length of each row represents the duration of each rotor, and the color shows its displacement across the atria. Raw and SRC ECGI signals show a similar number of rotors for each turn threshold (i.e. 0.5 turns, 169 vs 175 rotors respectively). In phase maps obtained both without filtering or with SRC, rotors last shorter and present longer trajectories than with NB HDF filtering.

As observed in Figs. 2-4, filtering, in general, tended to stabilize rotors, making them last longer and be less fragmented in time and space. Again, NB HDF filtering resulted in more stable rotors. A clear reduction in the number of rotors is shown when the duration threshold is increased as compared with less restrictive thresholds.

These findings can be further observed in the results from the whole population of 24 patients depicted in Fig. 5(a-c), where the mean and standard deviation values of two measurements of all metrics are presented. Raw signals presented very similar values compared to SRC filtering of SP/ms and spatial entropy. The number of SP/ms was significantly higher ($p < 0.01$) for NB HDF signals than for both raw or SRC signals (11.4 $\pm$ 8.07, 9.77 $\pm$ 6.89, and 9.4 $\pm$ 6.05, respectively, for 0.5 turns). By increasing the threshold for SP detection, the number of detected SP/ms decreased for the three filtering methods, although with more intensity for raw and SRC signals and for NB HDF to a lower extent.

Rotor duration, as depicted in Fig. 5(b), presented values under 0.2 s

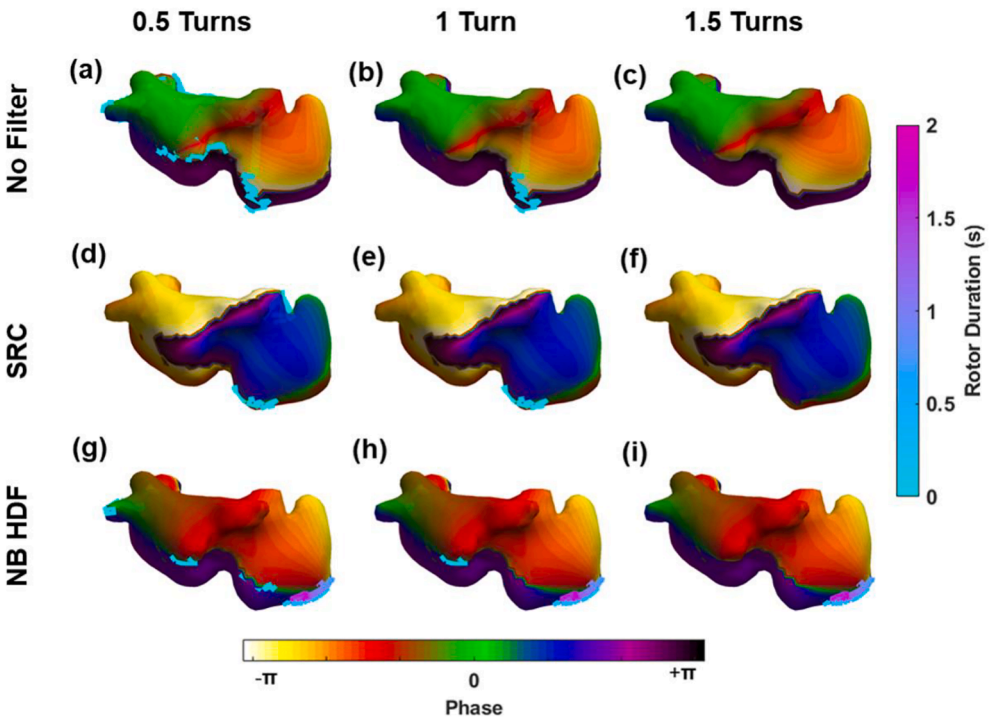

Fig. 2. Phase maps of an ECGI signal with different types of processing (no filter, sinusoidal Recomposition (SRC), and narrow band-pass filter at the highest dominant frequency (NB HDF) using different singularity point threshold detection 0.5, 1, and 1.5 turns. Colors projected on the atrial surface represent the instantaneous phase at the sample time instant. Lines depicted on top of the maps indicate the presence of rotors at the sample time instant blue-pink color indicates the evolution in time and space of each rotor. (For interpretation of the references to color in this figure legend, the reader is referred to the web version of this article.)

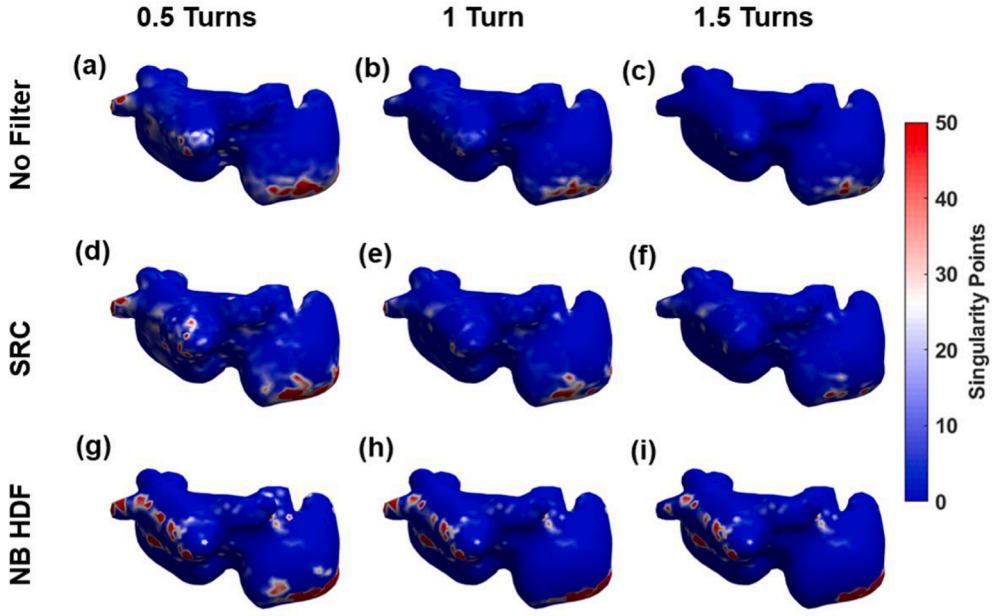

Fig. 3. Singularity point histogram of an ECGI signal with different types of processing (no filter, sinusoidal Recomposition (SRC), and narrow band-pass filter at the highest dominant frequency (NB HDF) using different singularity point threshold detection 0.5, 1, and 1.5 turns. The color projected on the atrial surface represents the number of rotors detected at each atrial site.

for raw signals. The duration was increased when filters were applied, especially in NB HDF filtered signals (1.5 turns SRC: 0.22 ± 0.07 s, HDF filtering: 0.47 ± 0.10 s). In addition, rotor duration presented increased values when thresholds were more restrictive (no filter at 0.5 turns: 0.07 ± 0.02 s, 1 turn: 0.1 ± 0.03 s and 1.5 turn: 0.14 ± 0.04 s). Therefore, both filtering and restrictive thresholds avoid the detection of reentrant patterns of shorter duration.

Spatial entropy presented fewer differences when filters were applied compared to other metrics. In this metric, the highest values were found for raw signals, with more similar results between SRC and NB HDF signals (1 turn: 9.23 ± 0.53, 8.68 ± 0.72, and 8.46 ± 0.69, respectively). Besides, spatial entropy showed lower values at higher turn thresholds. On the contrary, NB HDF filtered signals were not significantly decreased with restrictive thresholds (0.5 turns: 8.68 ± 0.66, 1 turn: 8.46 ± 0.69, and 1.5 turns: 8.23 ± 0.73). Overall, filtering and restrictive thresholds terminate with less complex SP histograms with lower spatial entropy.

In Fig. 5(d-f), the variability of each metric is presented for each post-processing alternative. Filtering did not reduce the temporal variability of the different metrics as it was expected, especially for NB HDF

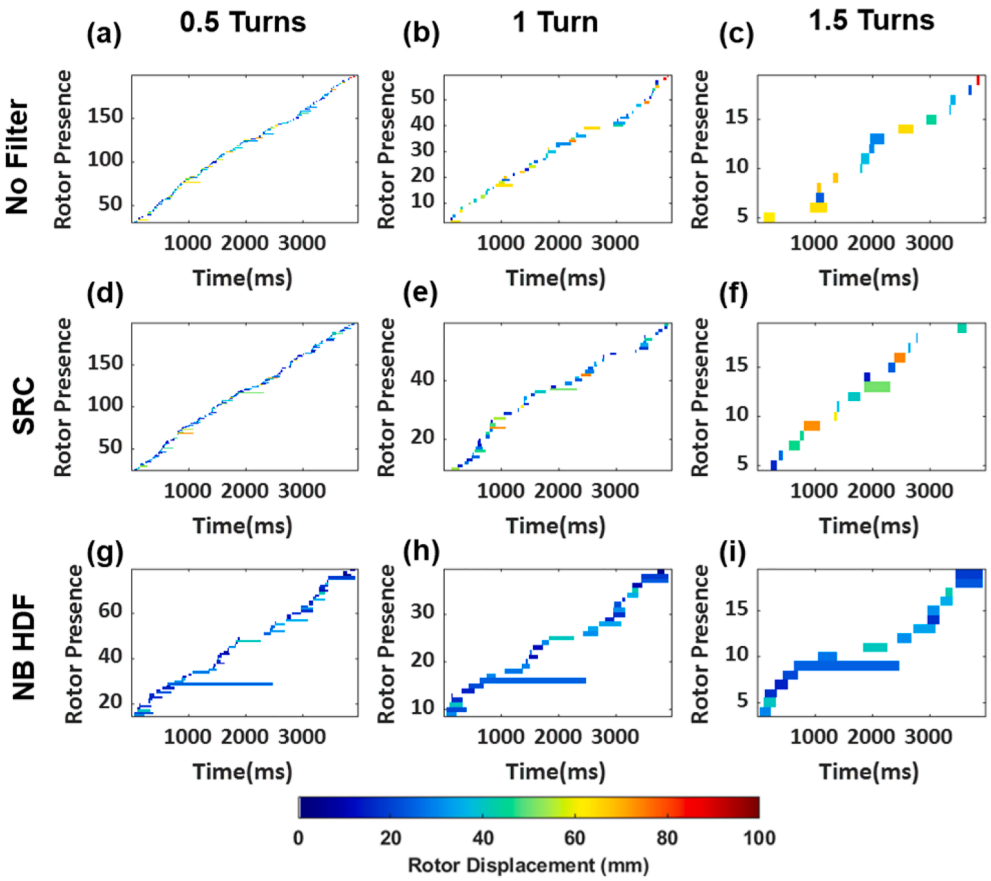

Fig. 4. Rotor presence during a 4-seconds recording with different types of processing (no filter, sinusoidal Recomposition (SRC), and narrow band-pass filter at the highest dominant frequency (NB HDF) using different singularity point threshold detection 0.5, 1, and 1.5 turns. Each row represents a rotor detected ordered by time at which each rotor first appears. Color represents the maximum rotor displacement.

filtering. In Fig. 5(d) it can be observed that ΔSP/ms presented similar results for raw and filtered signals, being decreased for higher turn thresholds. On the contrary, ΔSP/ms for NB HDF presented higher values, less affected by the turn threshold (1 turn raw: 13.8 ± 21.5 vs NB HDF: 25.5 ± 40.5). The ΔRduration was found to be lower in raw signals, showing low differences in the variability for the different thresholds. Nevertheless, the threshold on ΔRduration presented more drastic effects for the filtering signals, which presented rotors of more variable durations for higher turn thresholds. Finally, ΔEntropy showed higher values when the threshold increased, and higher variations between thresholds were seen for both raw (1 turn: 0.27 ± 0.29, 1.5 turns: 0.43 ± 0.46), and SRC filtered signals (1 turn: 0.38 ± 0.49, 1.5 turns: 0.58 ± 0.49).

3.2. *Post-processing effects and PVI outcome*

Values of the absolute difference between two metrics were compared between two groups of patients depending on their outcome 6 months after PVI. Fig. 6 shows boxplot diagrams of the quantified reentrant metrics for both the sinus and arrhythmia recurrence groups of patients. In general terms, patients with successful PVI at 6 months showed a lower variability of the metrics independently of the post-processing technique employed compared with patients with poor PVI outcome, although most of these differences were non-significant. The best post-processing alternative for discriminating between patients with a later successful PVI ablation was found to be raw signals and a duration threshold of 1 turn with p values for ΔRduration and ΔEntropy of 0.03 and 0.04, respectively).

Receiver operating characteristic curves were computed with the result of the univariate logistic regression of the normalized value of the combination of the variability of each alternative. In Fig. 7, ROC curves and area under the curve values are presented. The highest AUC value, 0.8, was found for raw signals with 1 turn threshold, which is consistent with the results displayed in Fig. 5. Both SRC and NB filtering were less successful for discriminating between patients with different outcomes, with the highest AUC equal to 0.71 and 0.62, respectively. Confusion matrices show that for the best AUC, a sensitivity of 100 % was obtained, with low values of specificity, that were higher in other post-processing alternatives that presented a worse general patient classification.

4. Discussion

In this paper, we present a comparison of different signal post-processing methods for reentrant activity detection in ECGI maps. We have shown that the interpretation of ECGI maps is dependent on the post-processing strategies employed, although results show that rotor location is stable and comparable between the proposed alternatives. The main findings of our work are that it is possible to find statistical differences in the variability of phase metrics obtained with ECGI recordings between patients with AF termination after PVI ablation and that those differences rely on the post-processing of ECGI signals before phase analysis.

We have shown that both sinusoidal recomposition and narrow band pass filtering centered at the HDF do stabilize phase singularities and make them easier to be tracked but reduce the differences in the variability of SP/ms, rotor duration, and the spatial entropy for different PVI outcome groups. The duration threshold for phase singularities to be considered has been shown to be of little relevance for the predictive power of phase-derived metrics.

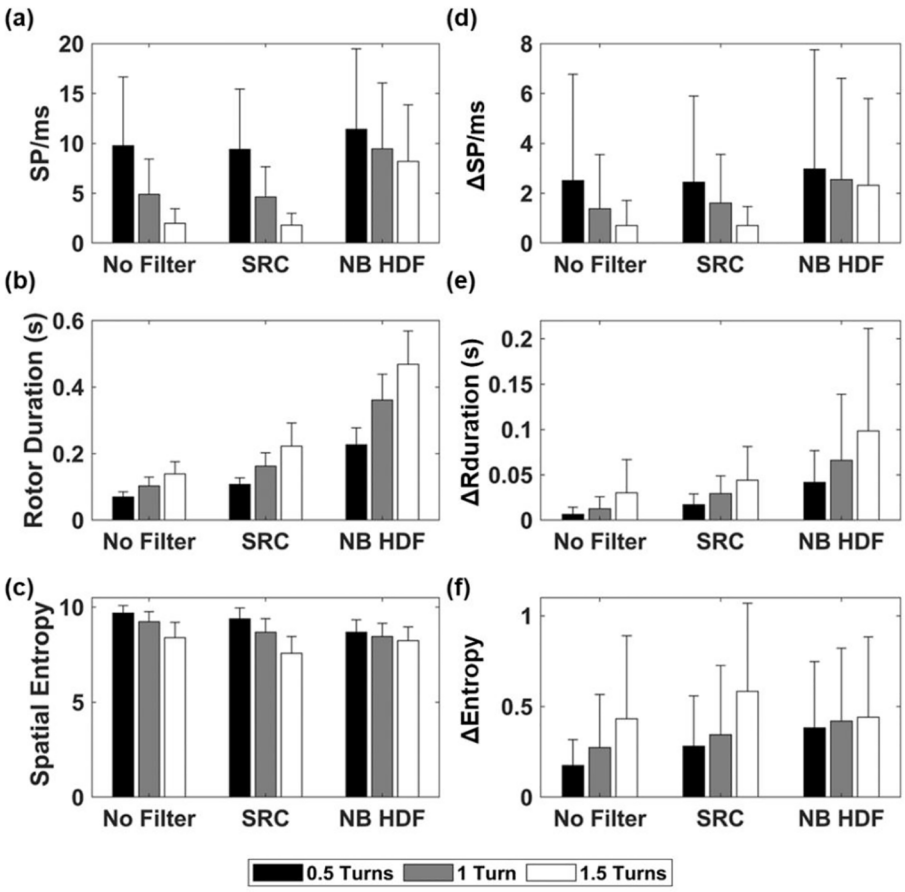

Fig. 5. Mean and standard deviation (a-c) values for each metric using different post-processing methods (no filter, sinusoidal Recomposition (SRC), and narrow band-pass filter at the highest dominant frequency (NB HDF) and different singularity points detection thresholds: 0.5 (black), 1 (gray) and 1.5 turns white). Variability between metrics extracted from two segments of each patient for the named post-processings (d-f).

4.1. ECGI-derived phase metrics and PVI outcome

We have found that rotor-derived metrics that best allow determining the differences between groups of patients depending on their PVI outcome are better found when no aggressive filters are applied prior to phase calculation in rotor duration and spatial entropy, especially when a traditional threshold of 1 turn was applied for the detection. Patients with a good PVI outcome presented lower variability between rotor duration and spatial entropy along time. A lower variability of the metrics can reflect a more stable atrial substrate with a better response to ablation treatments. Therefore, this may indicate that the detected rotors are related to the electrical substrate and are not just post-processing artifacts without a link to the atrial substrate of the patient. This observation of the patients with lower variability in the detected drivers is consistent with the success of therapies aiming at rotor elimination [2,3] that have shown an improved outcome by ablating AF sources since more stable in time reentrant activity can ease the AF termination.

In the logistic regression analysis, we observed consistent results with the individual metrics comparison. The resulting ROC curves of the study are moderate specially for SRC and NB-HDF filtering, with AUC values under 0.65 and a weak power of classification of the patients based on the PVI outcome. No filtering the ECGI signal and using a 1 turn SP detection threshold presented an AUC of 0.8 and could classify properly the totality of patients with good PVI response. Nevertheless, it was observed an increased number of patients with arrhythmia recurrence classified as PVI responders.

4.2. Effects of filtering ECGI signals for rotor detection

We have shown that filtering ECGI signals before applying the phase transform do impact the number of phase singularities detected and the resultant metrics. Filtering stabilized rotors but reduced the statistical differences between patients with different outcomes, especially for SRC filtering.

In previous studies from our group, we have used NB HDF filtering prior to phase singularity detections [5,9,17,18]. These studies show the potential of NB filtering in simulated and intracardiac electrograms of AF patients by stabilizing rotors that are unstable when using raw ECGI signals or the BSPM phase. We have also shown that HDF filtering applied to inverse computed simulated electrograms may cause artefactual rotors [9], which is consistent with the decreased discriminative power between patients with different outcomes compared to no filtered signals. No previous study has shown the effect of this filter on ECGI signals from AF patients. Even though it is not possible to know in a real case scenario which of our detected rotors are real and which rotors are artefactual, it is feasible that false rotor detection is also produced in real ECGI signals when HDF filter is applied. Nonetheless, the three different filtering approaches show equivalent results, being no filtering the signals the easier approach and more optimal for patient differentiation.

We have shown that the use of sinusoidal recomposition to detect reentrant activity in ECGI signals prior to SP detection does not improve rotor metrics as compared to the use of raw signals. Kuklik et al. showed that SRC filtering robustly alleviates the effect of noise on the phase of the signal [10], but it is not able to find a statistical difference in the variability of metrics between patients. In the same direction, more recent studies applying SRC to epicardial atrial electrograms have

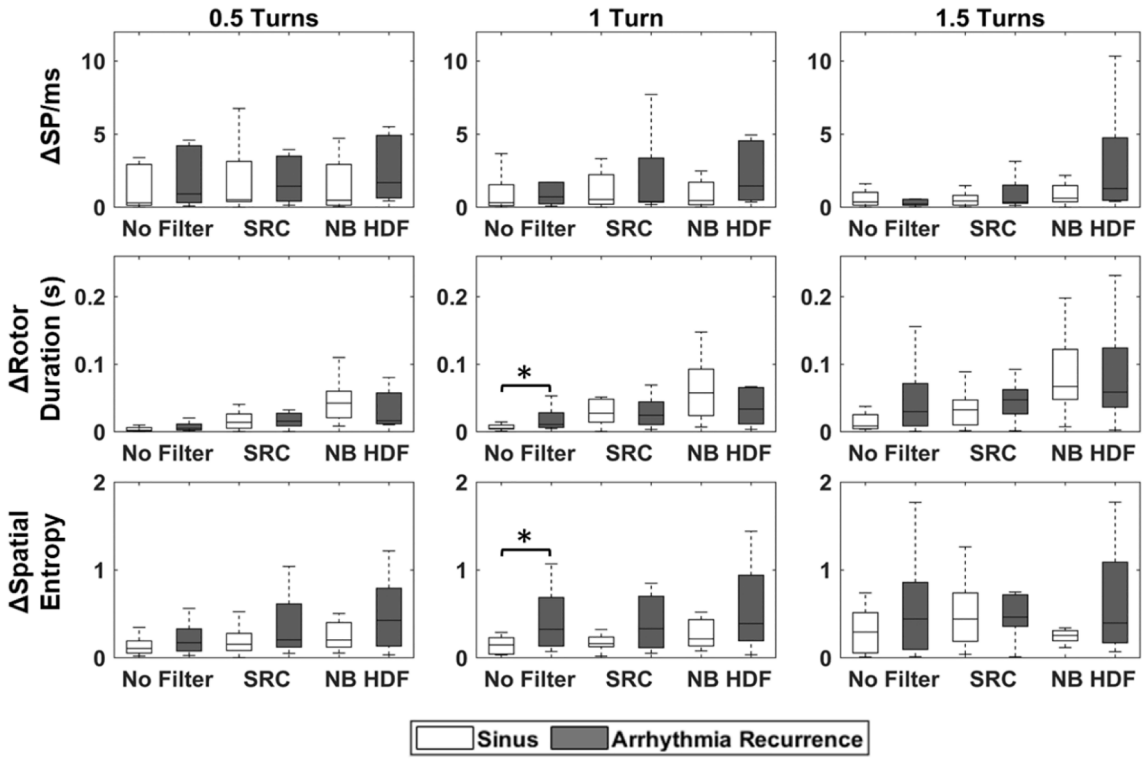

Fig. 6. Mean absolute difference between two measurements for reentrant metrics for patients classified by PVI outcome. Each row of panels represents each metric and each column of panels the thresholds used to detect a rotor. In each panel, on the left boxplots, no filtering is applied, middle: sinusoidal recomposition (SRC) and right: narrow band-pass filter at the highest dominant frequency (NB HDF). White boxplots represent patients with good PVI outcome, gray boxplots patients with bad PVI outcome. Outliers were removed for a better visualization of the results.

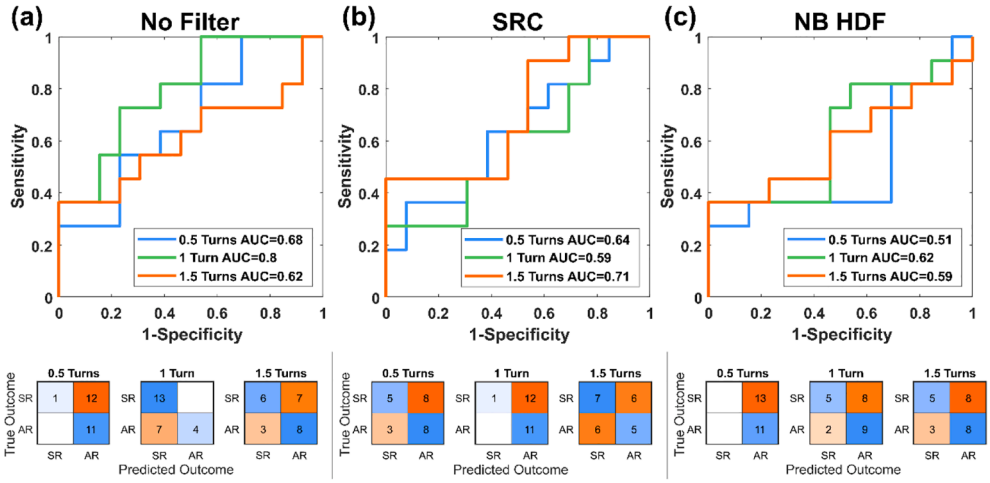

Fig. 7. Receiver operating characteristic curves and values of area under the curve (AUC) for the logistic regression with normalized mean variability of the three metrics for patients' classification based on PVI outcome for each filtering strategy and confusion matrices obtained with the optimal operating point of the ROC curve (SR: sinus rhythm, AR: arrhythmia recurrence). ROC curves obtained with 0.5, 1, and 1.5 phase singularities thresholds are presented in blue, green, and orange, respectively. (For interpretation of the references to color in this figure legend, the reader is referred to the web version of this article.)

shown that filtering the SPs had low specificity for identifying rotating wavefronts during human AF since lines of conduction block do result in phase singularities [19]. This is consistent with the presented results, which showed a decreased number of SP/ms when SRC was applied prior to rotor detection. The decreased value with the lower ability to differentiate patients per PVI outcome may indicate that SRC worsens the proper quantification of the real atrial substrate.

4.3. *Effects of time–space criteria for rotor detection*

In previous studies, we demonstrated that using 3 concentric rings to detect singularity points increases the sensitivity of reentrant activity identification [9] whereas others recommended only 2 for a robust detection [20]. Furthermore, SRC was applied to previous SP identification using 1 turn as threshold criteria [20,21]. Several authors [3,10,19] used this same threshold to consider a gradient of phase rotating a point in the atria to accept as a reentrant activity, but no consensus on this value has been established for ECGI signals of AF patients. Despite the lack of consensus, we showed a good correlation of noninvasive detected drivers with intracardiac mapping with a threshold of 1 turn [5].

The effect of establishing a duration threshold in the detection of rotors in patient signals has affected the discriminative power of the rotor metrics. In this study, we decided to test three different thresholds to detect SP. Better performance for longer and restrictive values (1.5 turns) was expected due to the elimination of spurious rotation

detections. In the present results, the threshold of 1 turn showed a better ability to differentiate relevant singularities to relate AF patients to their PVI outcome. This observation does not mean that there are no rotors that last less than one turn, but the propagation of this electrical pattern to the torso may hinder the tracking of the singularities, and more restrictive threshold values lose significant rotors. On the other hand, for thresholds lower than 1 turn, our results showed lower significance in the variability of the studied metrics.

4.4. Clinical implications

Pulmonary vein isolation has a 60 % success of AF termination [2], with higher success in patients with paroxysmal AF. For this reason, the inclusion criteria for this intervention mainly rely on AF patients' symptoms and AF classification [22]. Despite this, the low effectiveness of the ablation needs an improvement of the procedure and inclusion criteria of the patients. Other alternatives like rotor-driven ablation have demonstrated promising results in increasing AF termination compared to PVI only [2,3], nonetheless presence of rotors has not been used to predict AF ablation outcome [3]. The use of ECGI has been reported to be useful for rotor identification [5], and our study opens the possibility of using it as a clinical decision method to personalize treatments and as inclusion criteria for PVI to better select patients more likely to benefit from PVI. We present here a benchmark study to standardize the best post-processing methods for quantifying the presence of rotors in ECGI maps from patients with AF.

4.5. Limitations and future work

We have compared two aggressive filtering strategies of ECGI signals with a wide-band ECGI filtering and shown no benefits of filtering for identifying differences in rotor metrics related to PVI outcome. We cannot exclude the possibility that other post-processing methods could enhance significant differences in rotor metrics related to PVI outcome. Furthermore, the possibility of consideration of artifacts as rotors needs to be taken into account, as well as the possibility of considering that other possible mechanisms that may maintain AF could be detected after each filtering as wavelets [23].

It was not possible to determine the presence and location of rotors in intracardiac recordings because simultaneous intracardiac mapping with enough time–space resolution cannot be performed. For this reason, we have not been able to quantify the effect of post-processing techniques with intracavitary measurements as a gold standard, and we focused our study on finding significant differences between the variability of reentrant metrics from patients with different PVI outcomes.

5. Conclusion

Rotor metrics based on raw ECGI signals allow for differentiation of patients with different prognoses after pulmonary vein isolation. Aggressive filtering strategies of atrial ECGI signals are not necessary to identify relevant rotor features. A band-pass filtering of the signal before the inverse problem between 2 and 45 Hz is sufficient for proper differentiation between patients depending on their outcome based on phase-derived metrics. Additionally, to compute reentrant metrics, the threshold of 1 turn performed as the best alternative since it presents a compromise between not missing real detected rotors and not detecting just changes in the direction of the propagating wavefront.

CRediT authorship contribution statement

Rubén Molero: Conceptualization, Data curation, Formal analysis, Investigation, Visualization, Writing - original draft. **Ismael Hernández-Romero:** Visualization, Supervision. **Andreu M. Climent:** Supervision, Writing - review & editing. **María S. Guillem:** Conceptualization, Supervision, Writing - review & editing.

Declaration of Competing Interest

The authors declare that they have no known competing financial interests or personal relationships that could have appeared to influence the work reported in this paper.

Data availability

The authors do not have permission to share data.

Acknowledgments

The authors wish to thank Dr. Felipe Atienza for his support of the project and clinical advice.

Funding Sources

This work was supported in part by: Instituto de Salud Carlos III FEDER (Fondo Europeo de Desarrollo Regional PI17/01106), Agencia Estatal de Investigación (RYC2018-024346-I and PID2020-119364RB-100), Generalitat Valenciana Grants (ACIF/2020/265) and EIT Health (Activity code 19600). EIT Health is supported by EIT, a body of the European Union.

Disclosures

MS Guillem, A Climent and I. Hernández-Romero are co-founders and shareholders of CORIFY Inc.

References

[1] M.S. Guillem, A.M. Climent, M. Rogrido, F. Fernández-Avilés, F. Atienza, O. Berenfeld, Presence and stability of rotors in atrial fibrillation: Evidence and therapeutic implications, Cardiovasc. Res. 109 (4) (2010) 480–492, https://doi.org/10.1093/cvr/cvw011.

[2] S.M. Narayan, D.E. Krummen, K. Shivkumar, P. Clopton, W.J. Rappel, J.M. Miller, Treatment of atrial fibrillation by the ablation of localized sources: CONFIRM (Conventional Ablation for Atrial Fibrillation with or Without Focal Impulse and Rotor Modulation) trial, J. Am. Coll. Cardiol. 60 (7) (2012) 628–636, https://doi.org/10.1016/j.jacc.2012.05.022.

[3] M. Haissaguerre, M. Hocini, A. Denis, A.J. Shah, Y. Komatsu, S. Yamashita, M. Daly, S. Amraoui, S. Zellerhoff, M.Q. Picat, A. Quotb, L. Jesel, H. Lim, S. Ploux, P. Bordachar, G. Attuel, V. Meillet, P. Ritter, N. Derval, F. Sacher, O. Bernus, H. Cochet, P. Jais, R. Dubois, Driver domains in persistent atrial fibrillation, Circulation 130 (2014) 530–538, https://doi.org/10.1161/CIRCULATIONAHA.113.005421.

[4] M. Haissaguerre, M. Hocini, A.J. Shah, N. Derval, F. Sacher, P. Jais, R. Dubois, Noninvasive panoramic mapping of human atrial fibrillation mechanisms: A feasibility report, J. Cardiovasc. Electrophysiol. 24 (6) (2013) 711–717, https://doi.org/10.1111/jce.12075.

[5] M. Rodrigo, A.M. Climent, I. Hernández-Romero, A. Liberos, T. Baykaner, A. J. Rogers, M. Alhusseini, P.J. Wang, F. Fernández-Avilés, M.S. Guillem, S. M. Narayan, F. Atienza, Non-invasive assessment of complexity of atrial fibrillation: correlation with contact mapping and impact of ablation, Circ. Arrhythmia Electrophysiol. 13 (3) (2020) e007700, https://doi.org/10.1161/CIRCEP.119.007700.

[6] S. Zlochiver, M. Yamazaki, J. Kalifa, O. Berenfeld, Rotor meandering contributes to irregularity in electrograms during atrial fibrillation, Hear. Rhythm. 5 (6) (2008) 846–854, https://doi.org/10.1016/j.hrthm.2008.03.010.

[7] S.M. Narayan, D.E. Krummen, M.W. Enyeart, W.J. Rappel, Computational mapping identifies localized mechanisms for ablation of atrial fibrillation, PLoS One 7 (9) (2012) 1–8, https://doi.org/10.1371/journal.pone.0046034.

[8] M. Rodrigo, A.M. Climent, A. Liberos, F. Fernández-Avilés, O. Berenfeld, F. Atienza, M.S. Guillem, Highest dominant frequency and rotor positions are robust markers of driver location dring noninvasive mapping of atrial fibrillation: A computational study, Hear Rhythm. 14 (8) (2017) 1224–1233, https://doi.org/10.1016/j.hrthm.2017.04.017.

[9] M. Rodrigo, A.M. Climent, A. Liberos, F. Fernández-Avilés, O. Berenfeld, F. Atienza, M.S. Guillem, Technical considerations on phase mapping for identification of atrial reentrant activity in direct- and inverse-computed electrograms, Circ. Arrhythmia Electrophysiol. 10 (9) (2017) e005008, https://doi.org/10.1161/circep.117.005008.

[10] P. Kuklik, S. Zeemering, B. Maesen, J. Maessen, H.J. Crijns, S. Verheule, A. N. Ganesan, U. Schotten, Reconstruction of instantaneous phase of unipolar atrial

contact electrogram using a concept of sinusoidal recomposition and Hilbert transform, IEEE Trans. Biomed. Eng. 62 (1) (2015) 296–302, https://doi.org/10.1109/TBME.2014.2350029.

[11] R. Molero, A.M. Climent, M.S. Guillem, Post-processing of electrocardiographic imaging signals to identify atrial fibrillation drivers, Computing in Cardiology. 47 (2020) 1–4. https://doi.org/10.22489/CinC.2020.113.

[12] R. Molero, J.M. Soler Torro, N. Martínez Alzamora, A.M. Climent, M.S. Guillem, Higher reproducibility of phase derived metrics from electrocardiographic imaging during atrial fibrillation in patients remaining in sinus rhythm after pulmonary vein isolation, Comput. Biol. Med. 139 (2021), 104934, https://doi.org/10.1016/j.compbiomed.2021.104934.

[13] F. Remondino, 3-D reconstruction of static human body shape from image sequence, Comput. Vis. Image Underst. 93 (1) (2004) 65–85, https://doi.org/10.1016/j.cviu.2003.08.006.

[14] P.A. Yushkevich, H. Zhang, J.C. Gee, Continuous medial representation for anatomical structures, IEEE Trans. Med. Imaging. 25 (12) (2006) 1547–1564, https://doi.org/10.1109/TMI.2006.884634.

[15] F. Castells, C. Mora, J.J. Rieta, D. Moratal-Pérez, J. Millet, Estimation of atrial fibrillatory wave from single-lead atrial fibrillation electrocardiograms using principal component analysis concepts, Med. Biol. Eng. Comput. 43 (2005) 557–560, https://doi.org/10.1007/BF02351028.

[16] M. Rodrigo, M.S. Guillem, A.M. Climent, A. Liberos, I. Hernández-Romero, Á. Arenal, J. Bermejo, F. Fernández-Avilés, F. Atienza, M.S. Guillem, Solving inaccuracies in anatomical models for electrocardiographic inverse problem resolution by maximizing reconstruction quality, IEEE Trans. Med. Imaging. 37 (3) (2018) 733–740, https://doi.org/10.1109/TMI.2017.2707413.

[17] M. Rodrigo, M.S. Guillem, A.M. Climent, J. Pedrón-Torrecilla, A. Liberos, J. Millet, F. Fernández-Avilés, F. Atienza, O. Berenfeld, Body surface localization of left and right atrial high-frequency rotors in atrial fibrillation patients: A clinical-computational study, Hear. Rhythm. 11 (9) (2014) 1584–1591, https://doi.org/10.1016/j.hrthm.2014.05.013.

[18] A. Costoya-Sánchez, A.M. Climent, I. Hernández-Romero, A. Liberos, F. Fernández-Avilés, S.M. Narayan, F. Atienza, M.S. Guillem, M. Rodrigo, Automatic quality electrogram assessment improves reentrant activity identification in atrial fibrillation, Comput. Biol. Med. 117 (2020), https://doi.org/10.1016/j.compbiomed.2019.103593.

[19] P. Podziemski, S. Zeemering, P. Kuklik, A. van Hunnik, B. Maesen, J. Maessen, H. J. Crijns, S. Verheule, U. Schotten, Rotors detected by phase analysis of filtered, epicardial atrial fibrillation electrograms colocalize with regions of conduction block, Circ. Arrhythm. Electrophysiol. 11 (10) (2018) e005858, https://doi.org/10.1161/CIRCEP.117.005858.

[20] P. Kuklik, S. Zeemering, A. van Hunnik, B. Maesen, L. Pison, D.H. Lau, J. Maessen, P. Podziemski, C. Meyer, B. Schäffer, H. Crijns, S. Willems, U. Schotten, Identification of rotors during human atrial fibrillation using contact mapping and phase singularity detection: technical considerations, IEEE Trans. Biomed. Eng. 64 (2) (2017) 310–318, https://doi.org/10.1109/TBME.2016.2554660.

[21] D. Dharmaprani, M. Schopp, P. Kuklik, D. Chapman, A. Lahiri, L. Dykes, F. Xiong, M. Aguilar, B. Strauss, L. Mitchell, K. Pope, C. Meyer, S. Willems, F.G. Akar, S. Nattel, A.D. McGavigan, A.N. Ganesan, Renewal theory as a universal quantitative framework to characterize phase singularity regeneration in mammalian cardiac fibrillation, Circ. Arrhythmia Electrophysiol. 12 (12) (2019) 1–12, https://doi.org/10.1161/CIRCEP.119.007569.

[22] G. Hindricks, T. Potspara, N. Dagres, E. Arbelo, J.J. Bax, C. Blomström-Lundqvist, G. Boriani, M. Castella, G.-A. Dan, P.E. Dilaveris, L. Fauchier, G. Filippatos, J. M. Kalman, M. La Meir, D.A. Lane, J.P. Lebeau, 2020 ESC Guidelines for the diagnosis and management of atrial fibrillation developed in collaboration with the European Association of Cardio-Thoracic Surgery (EACTS), Eur. Heart J. 42 (2021) 373–498, https://doi.org/10.1093/eurheartj/ehaa612.

[23] U. Schotten, S. Lee, S. Zeemering, A.L. Waldo, Paradigm shifts in electrophysiological mechanisms of atrial fibrillation, Europace 23 (2021) II9–II13, https://doi.org/10.1093/europace/euaa384.